Asymptotic Backstepping Stabilization of an Underactuated Surface Vessel

Jawhar Ghommam, *Student Member, IEEE*, Faïçal Mnif, *Senior Member, IEEE*, Abderraouf Benali, and Nabil Derbel, *Senior Member, IEEE*

***Abstract*—This brief addresses the problem of controlling the planar position and orientation of an autonomous underactuated surface vessel. Under realistic assumptions, we show, first, that there exists a natural change of coordinates that transforms the whole dynamical system into a cascade nonlinear system, and, second, the control problem of the resulting system can be reduced to the stabilization of a third-order chained form. A time-invariant discontinuous feedback law is derived to guarantee global uniform asymptotic stabilization of the system to the desired configuration. The construction of such a controller is based on the backstepping design approach. A simulation example is included to demonstrate the effectiveness of the suggested approach.**

***Index Terms*—Backstepping stabilization, chained forms, discontinuous control, nonholonomic constraints, nonlinear cascade systems, underactuated surface vessels.**

I. Introduction

UNDERACTUATED vehicles have fewer independent control actuators than degrees-of-freedom (DOF) to be controlled. Underactuation could be due to an actuator failure or by deliberate design decision [7], motivated by weight and cost constraint considerations. Fault tolerance to actuator failures could be achieved by equipping the vehicle with redundant actuators. However, a less costly option could be achieved by switching to a control law that controls the vehicle using only the remaining actuators [4]. The control solution, regardless of the reason of underactuation, is often weight economical compared to the hardware solution, and this could be an important issue in space and water applications [5]. Dynamic models of underactuated vehicles result in systems with second-order nonholonomic constraints.

Stabilization of underactuated surface vessels has been tackled in a number of research studies in the last few years [6], [11], [16]–[19], [21]. The authors in [21] have shown that the dynamics of underactuated vehicles do not satisfy Brocket's necessary condition [2] if the unactuated dynamics contain no gravitational field component. In this case, the vehicles are not asymptotically able to stabilize to a desired equilibrium solution using time-invariant continuous feedback laws. Wichlund *et al.* [21] have proposed a continuous feedback control law that asymptotically stabilizes an equilibrium manifold. The desired equilibrium point is stable in the sense that all the system's variables are bounded by the initial conditions of the system. Furthermore, the position variables converge exponentially to their desired values. The course angle, however, converges to some constant value, but not necessarily to zero. In [19], a discontinuous feedback control law has been discussed for the exponential convergence of the equilibrium point under certain assumptions on the variables initial value. In [17], a time-varying feedback control law has suggested, and which provides exponential (with respect to a given dilation) stability of the desired equilibrium point. However, the feedback law only locally stabilizes the desired equilibrium point, and the size of the region of attraction is not known. The authors in [18] have presented a time-varying feedback control law that provides semiglobal practical exponential stability of a simplified model of the ship, where the surge and yaw velocities are considered as controls. In [6], another simplified ship model has been examined (the hovercraft) based on passivity considerations and Lyapunov theory, discontinuous control laws have been derived to ensure the global convergence to the origin.

This brief considers the problem of controlling the planar position and orientation of an autonomous surface vessel using two independent side thrusters. Two transformations are introduced to represent the system into a pure cascade form. We show through some key properties of the model that the global and uniform asymptotic stabilization problem of the resulting cascade system can be reduced to the stabilization problem of a third-order chained form. A discontinuous backstepping approach is then employed for the stabilization of the chained form system via a partial state feedback. We show that the proposed control law exponentially stabilizes the reduced model in a defined set, ensuring the uniform global asymptotic stabilization of the underactuated surface vessel model. One of the desirable features of the suggested approach is that it provides a systematic procedure to transform a class of nonholonomic dynamical systems into a nonlinear cascade form. Such representation opens the possibility of developing more constructive control tools than those already existing in the literature, e.g., [6], [16]–[19]. The discontinuity involved in our design is not as restrictive as in [19], since it only conditions one initial state to be nonzero. Unlike [6], our proposed approach does not generate any oscillatory and/or chattering behavior to the output/control variables. Simulation results show that the dynamic performances of the closed-loop system are satisfactory.

The remainder of this brief is organized as follows. Section II introduces the nonlinear control system and describes the dynamics of the underactuated surface vessel. Section III describes a change of the system's coordinates, and then the design of a

Manuscript received February 23, 2006. Manuscript received in final form May 24, 2006. Recommended by Associate Editor C. Rabbath.

J. Ghommam is with the Intelligent Control Design and Optimization of Complex Systems Unit Ecole Nationale d'Ingenieurs de Sfax, Route Soukra km 3.5 BP 3038, Tunisia, and is also with the Laboratoire de Vision et Robotique (UPRES EA 2078), 18000 Bourges, France (e-mail: jawhar.ghommam@ieee.org).

F. Mnif and N. Derbel are with the Intelligent Control Design and Optimization of Complex Systems Unit Ecole Nationale d'Ingenieurs de Sfax, Route Soukra km 3.5 BP 3038, Tunisia (e-mail: mnif@ieee.org; nabil.derbel@ieee.org).

A. Benali is with the Laboratoire de Vision et Robotique (UPRES EA 2078), 18000 Bourges, France (e-mail: abderraouf.benali@ensi-bourges.fr)

Digital Object Identifier 10.1109/TCST.2006.880220

globally asymptotically stabilizing controller using a discontinuous feedback law. Section IV presents a simulation example and discusses the obtained results. Finally, Section V concludes this study and provides possible directions for future work.

II. Ship Model

A. Kinematic Model

Marine vessels require six independent coordinates to determine their complete configuration (position and orientation). The six different motion components are conveniently defined as surge, sway, heave, roll, pitch, and yaw. It is common to reduce the general six-DOF of the model to motion in surge, sway, and yaw only. This is done by neglecting the heave, roll, and pitch modes which are open loop stable for most ships. The state vector $\boldsymbol{\eta} \in \mathbf{SE}(2)$ is then defined by

$$\boldsymbol{\eta} = [x, y, \psi]^\top \tag{1}$$

where $(x, y) \in \mathbb{R}^2$ is the position of the ship given in an inertial frame, and $\psi \in [0, 2\pi)$ is the heading angle of the ship relative to the geographic North.

The kinematic model resulting from the nonholonomic constraints can be written as

$$\dot{\boldsymbol{\eta}} = \mathbf{R}(\boldsymbol{\psi})\boldsymbol{\nu} \tag{2}$$

where $\mathbf{R}$ is the rotation matrix in yaw and $\nu \in \mathbb{R}^3$ is a vector containing the linear body-fixed velocities. $\mathbf{R}$ is defined as

$$\mathbf{R}(\psi) = \begin{pmatrix} \cos\psi & -\sin\psi & 0 \\ \sin\psi & \cos\psi & 0 \\ 0 & 0 & 1 \end{pmatrix} \tag{3}$$

with the property $\mathbf{R}^\top = \mathbf{R}^{-1}$. The velocity vector $\boldsymbol{\nu}$ is defined by

$$\boldsymbol{\nu} = [u, v, r]^\top. \tag{4}$$

Here, u is the forward velocity (surge), v is the transverse velocity (sway), and r is the angular velocity in yaw decomposed in the body-fixed frame (see Fig. 1).

B. Dynamic Model

The dynamic ship model used in this brief is based on [8]. The model describes the motion of the ship in surge, sway, and yaw. Denote the control forces in surge and sway, and the yaw moment by $\boldsymbol{\tau}$. Hence, the nonlinear ship model is given by

$$\mathbf{M}(\boldsymbol{\nu})\dot{\boldsymbol{\nu}} + \mathbf{B}(\boldsymbol{\nu}) = \boldsymbol{\tau} + \mathbf{R}^\top\mathbf{b} \tag{5}$$

where the Coriolis and centripetal matrix $\mathbf{C}$ and damping matrix $\mathbf{D}$ are collected into a vector $\mathbf{B}$ given by

$$\mathbf{B}(\boldsymbol{\nu}) = \mathbf{C}(\boldsymbol{\nu})\boldsymbol{\nu} + \mathbf{D}(\boldsymbol{\nu})\boldsymbol{\nu} \tag{6}$$

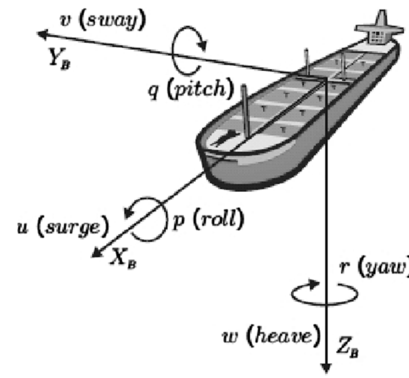

Fig. 1. Vessel motion variable.

where $\mathbf{R}^\top\mathbf{b}\in\mathbb{R}^3$ describes the low-frequency environmental forces acting on the vessel, e.g., wind, wave loads, and current. Combining (2) and (5), we obtain the complete kinematical and dynamical vector equation describing the motion of a surface vessel

$$\mathbf{M}(\boldsymbol{\nu})\dot{\boldsymbol{\nu}} + \mathbf{C}(\boldsymbol{\nu})\boldsymbol{\nu} + \mathbf{D}(\boldsymbol{\nu})\boldsymbol{\nu} = \boldsymbol{\tau} + \mathbf{R}^\top\mathbf{b} \tag{7}$$

$$\dot{\boldsymbol{\eta}} = \mathbf{R}(\psi)\boldsymbol{\nu}. \tag{8}$$

To simplify the analysis in the following sections, we make the following assumptions.

A1: The inertia matrix $\mathbf{M}$ and the damping matrix $\mathbf{D}$ are assumed to be diagonal: $\mathbf{M} = \mathrm{diag}(m_{11}, m_{22}, m_{33})$, $\mathbf{D} = \mathrm{diag}(d_{11}, d_{22}, d_{33})$.

A2: We neglect the effect of disturbance forces, that is $\mathbf{R}^\top\mathbf{b}\approx\mathbf{0}$.

Since the ship is considered to be underactuated, we will only consider the two available control inputs that are in surge and yaw directions: i.e., $\boldsymbol{\tau} = [\boldsymbol{\tau}_1, 0, \boldsymbol{\tau}_3]^\top$.

The Coriolis matrix $\mathbf{C}(\boldsymbol{\nu})$ has the following form [8]:

$$\mathbf{C}(\boldsymbol{\nu}) = \begin{bmatrix} 0 & 0 & -m_{22}v \\ 0 & 0 & m_{11}u \\ m_{22}v & -m_{11}u & 0 \end{bmatrix}. \tag{9}$$

After simple algebraic manipulations, the dynamics (7)–(8) are found to be

$$\dot{\boldsymbol{\eta}} = \mathbf{R}(\psi)\boldsymbol{\nu} \tag{10}$$

$$\dot{\boldsymbol{u}} = \frac{m_{22}}{m_{11}}vr - \frac{d_{11}}{m_{11}}u + \frac{1}{m_{11}}\tau_1 \tag{11}$$

$$\dot{\boldsymbol{v}} = -\frac{m_{11}}{m_{22}}ur - \frac{d_{22}}{m_{22}}v \tag{12}$$

$$\dot{\boldsymbol{r}} = \frac{m_{11} - m_{22}}{m_{33}}uv - \frac{d_{33}}{m_{33}}r + \frac{1}{m_{33}}\tau_3. \tag{13}$$

III. Global Stabilization of an Underactuated Surface Vessel

Proposition 3.1: There exists no continuous time-invariant state feedback that renders the system (10)–(13) asymptotically stable about the origin.

Proof: (See Proposition 2.3 in [16] for a similar proof). ■

Since the system (10)–(13) is real analytic, there exists a piecewise analytic feedback law which can stabilize the closed-loop system to a given equilibrium [20].

In this section, we will consider the problem of designing a discontinuous feedback control law for the system (10)–(13). We first propose the following global diffeomorphism change of coordinate

$$z = \mathbf{R}^\top \boldsymbol{\eta} \tag{14}$$

where $\mathbf{z} = [\mathbf{z}_1, \mathbf{z}_2, \mathbf{z}_3]^\top$ and $\boldsymbol{\eta} = [x, y, \psi]^\top$. Taking the derivative of (14), we can write

$$\dot{z} = \dot{\boldsymbol{R}}^\top \boldsymbol{\eta} + \mathbf{R}^\top \dot{\boldsymbol{\eta}}. \tag{15}$$

Noting

$$\dot{\mathbf{R}} = \mathbf{R}\widehat{\mathbf{r}} \tag{16}$$

with

$$\widehat{\mathbf{r}} = \begin{bmatrix} 0 & -r & 0 \\ r & 0 & 0 \\ 0 & 0 & 1 \end{bmatrix}. \tag{17}$$

Equation (15) becomes

$$\begin{aligned} \dot{z} &= \widehat{\mathbf{r}}^\top \mathbf{R}^\top \boldsymbol{\eta} + \mathbf{R}^\top \dot{\boldsymbol{\eta}} && (18) \\ &= \widehat{\mathbf{r}}^\top \mathbf{R}^\top \boldsymbol{\eta} + \mathbf{R}^\top \mathbf{R} v. && (19) \end{aligned}$$

The state equations of the surface vessel are then found as

$$\begin{bmatrix} \dot{\mathbf{z}} \\ \dot{\boldsymbol{\nu}} \end{bmatrix} = \begin{bmatrix} \widehat{\mathbf{r}}^\top \mathbf{R}^\top \boldsymbol{\eta} \\ \mathbf{M}^{-1}(\tau - \mathbf{C}(\boldsymbol{\nu})\boldsymbol{\nu} - \mathbf{D}(\boldsymbol{\nu})\boldsymbol{\nu}) \end{bmatrix} + \begin{bmatrix} \boldsymbol{\nu} \\ \mathbf{0}_{3\times 1} \end{bmatrix}. \tag{20}$$

The state (20), can be explicitly written as

$$\begin{aligned} \dot{\mathbf{z}}_1 &= u + \mathbf{z}_2 r && (21) \\ \dot{\mathbf{z}}_2 &= v - \mathbf{z}_1 r && (22) \\ \dot{\mathbf{z}}_3 &= r && (23) \\ \dot{u} &= \frac{m_{22}}{m_{11}} vr - \frac{d_{11}}{m_{11}} u + \frac{1}{m_{11}} \tau_1 && (24) \\ \dot{v} &= -\frac{m_{11}}{m_{22}} ur - \frac{d_{22}}{m_{22}} v && (25) \\ \dot{r} &= \frac{m_{11} - m_{22}}{m_{33}} uv - \frac{d_{33}}{m_{33}} r + \frac{1}{m_{33}} \tau_3. && (26) \end{aligned}$$

A. State Transformation

For the sake of compactness of the model, we propose the following transformation:

$$\begin{aligned} \tau_u &= \frac{m_{22}}{m_{11}} vr - \frac{d_{11}}{m_{11}} u + \frac{1}{m_{11}} \tau_1 && (27) \\ \tau_r &= \frac{m_{11} - m_{22}}{m_{33}} uv - \frac{d_{33}}{m_{33}} r + \frac{1}{m_{33}} \tau_3. && (28) \end{aligned}$$

Letting $\mathbf{A} = m_{11}/m_{22}$ and $\mathbf{B} = d_{22}/m_{22}$, the dynamics (24)–(26) become

$$\begin{cases} \dot{u} = \tau_u \\ \dot{v} = -\mathbf{A}ur - \mathbf{B}v \\ \dot{r} = \tau_r. \end{cases} \tag{29}$$

In order to remove the underactuated variable v from the dynamic (22), following [11], we propose a new coordinate variable $\mathbf{Z}_2$ such that

$$\mathbf{Z}_2 = \mathbf{z}_2 + \frac{v}{\mathbf{B}} \tag{30}$$

the $(\mathbf{z}_1, \mathbf{Z}_2)$-subsystem dynamics can be expressed as

$$\begin{aligned} \dot{\mathbf{z}}_1 &= u + \mathbf{Z}_2 r - \frac{v}{\mathbf{B}} r && (31) \\ \dot{\mathbf{Z}}_2 &= -\frac{\mathbf{A}}{\mathbf{B}} ur - \mathbf{z}_1 r. && (32) \end{aligned}$$

We now introduce a virtual control input α such that

$$u = -\frac{\mathbf{B}}{\mathbf{A}}(\mathbf{z}_1 + \boldsymbol{\alpha}). \tag{33}$$

This leads to the following system:

$$\begin{aligned} \dot{\mathbf{z}}_1 &= -\frac{\mathbf{B}}{\mathbf{A}}\mathbf{z}_1 - \frac{\mathbf{B}}{\mathbf{A}}\boldsymbol{\alpha} + \left(\mathbf{Z}_2 - \frac{v}{\mathbf{B}}\right) r && (34) \\ \dot{\mathbf{Z}}_2 &= \boldsymbol{\alpha} r && (35) \\ \dot{\mathbf{z}}_3 &= r && (36) \\ \dot{v} &= -\mathbf{B}v + \mathbf{B}(\mathbf{z}_1 + \boldsymbol{\alpha}) r && (37) \\ \dot{\boldsymbol{\alpha}} &= \tau_\alpha, \qquad \dot{r} = \tau_r && (38) \end{aligned}$$

where

$$\tau_\alpha = \frac{B}{A}(\mathbf{z}_1 + \alpha) - r(\mathbf{Z}_2 - \frac{v}{B}) - \frac{A}{B}\tau_u$$

B. Cascade Nonlinear System

The system (34)–(38) can be viewed as two interconnected subsystems in cascade form that can be written as follows:

$$\begin{aligned} \sum_1 &: \dot{\mathbf{x}}_1 = \mathbf{f}_1(t, \mathbf{x}_1) + \mathbf{G}(t, \mathbf{x})\mathbf{x}_2 && (39) \\ \sum_2 &: \dot{\mathbf{x}}_2 = \mathbf{f}_2(t, \mathbf{x}_2, \mathbf{u}). && (40) \end{aligned}$$

where $\mathbf{x}_1 \triangleq [\mathbf{z}_1, v], \mathbf{x}_2 \triangleq [\mathbf{Z}_2, z_3, \alpha, r], \mathbf{x} \triangleq [\mathbf{x}_1, \mathbf{x}_2]$. The function $\mathbf{f}_1(t, \mathbf{x}_1)$ is continuously differentiable in $(t, \mathbf{x}_1)$ and $\mathbf{f}_2(t, \mathbf{x}_2, \mathbf{u}), \mathbf{G}(t, \mathbf{x})$ are continuous in their arguments and locally Lipschitz.

Theorem 4.1 [15] (UGAS of a Cascade System): The cascade system $\sum_1$ and $\sum_2$, given by (39)–(40) is globally uniformly asymptotically stable if the following are met.

1) The system $\dot{\mathbf{x}}_1 = f_1(t, \mathbf{x}_1)$ is uniformly globally asymptotically stable.
2) There exists a control law u that globally asymptotically stabilizes the system $\sum_2$.
3) The function $\mathbf{G}(t, \mathbf{x})$ satisfies

$$\|\mathbf{G}(t, \mathbf{x})\|_2 \le \theta_1(\|x_2\|_2) + \theta_2(\|x_2\|_2)\|x_1\|_2. \tag{41}$$

Equations (34)–(38) can be put under the form (39)–(40), where

$$\mathbf{f}_1(t,\mathbf{x}_1)+\mathbf{G}(t,\mathbf{x})\mathbf{x}_2=\begin{bmatrix}-\frac{\mathbf{B}}{\mathbf{A}}\mathbf{z}_1-\frac{\mathbf{B}}{\mathbf{A}}\boldsymbol{\alpha}+(\mathbf{Z}_2-\frac{v}{\mathbf{B}})r\\ -\mathbf{B}v+\mathbf{B}(\mathbf{z}_1+\boldsymbol{\alpha})r\end{bmatrix} \tag{42}$$

$$\mathbf{f}_2(t,\mathbf{x}_2,\mathbf{u})=[\boldsymbol{\alpha}r \quad r \quad \tau_\alpha \quad \tau_r]^\top. \tag{43}$$

Proposition 4.1: For the dynamic underactuated ship model, the transformed subsystem $\mathbf{f}_1(t,\mathbf{x}_1)$ given by

$$\mathbf{f}_1(t,\mathbf{x}_1)\triangleq=\begin{bmatrix}-\frac{\mathbf{B}}{\mathbf{A}}\mathbf{z}_1\\ -\mathbf{B}v\end{bmatrix} \tag{44}$$

is globally exponentially stable.

Proof: System (44) is linear with strictly negative time invariant eigenvalues given by $\lambda_1=-\mathbf{B}/\mathbf{A}=-d_{22}/m_{11}$ and $\lambda_2=-\mathbf{B}=-d_{22}/m_{22}$. ■

Proposition 4.2: The Component $\mathbf{G}(t,\mathbf{x})$ in $\mathbf{G}(t,\mathbf{x})x_2$ given by

$$\mathbf{G}(t,\mathbf{x})\mathbf{x}_2\triangleq\begin{bmatrix}-\frac{\mathbf{B}}{\mathbf{A}}\boldsymbol{\alpha}+(\mathbf{Z}_2-\frac{v}{\mathbf{B}})r\\ \mathbf{B}(\mathbf{z}_1+\boldsymbol{\alpha})r\end{bmatrix} \tag{45}$$

satisfies a norm upper bound limit in the form

$$\|\mathbf{G}(t,\mathbf{x})\|_2\le\theta_1\|\mathbf{x}_2\|_2+\theta_2(\|\mathbf{x}_2\|_2)\|\mathbf{x}_1\|_2 \tag{46}$$

where $\theta_1=\max(\mathbf{B},1/\mathbf{B})$, and $\theta_2(\|x_2\|_2)=(\mathbf{B}+1)\|x_2\|_2+\mathbf{B}/\mathbf{A}\cdot\|\cdot\|_2$ refers to the Euclidian norm defined for vectors and the induced Euclidian norm defined for matrices.

Proof: The function $\mathbf{G}(t,\mathbf{x})$ can be written as follows:

$$\mathbf{G}(t,\mathbf{x})\triangleq\left[\left[r,0,-\frac{\mathbf{B}}{\mathbf{A}},-\frac{v}{\mathbf{B}}\right]^\top,[0,0,\mathbf{B}r,\mathbf{B}\mathbf{z}_1]^\top\right]^\top$$

hence

$$\begin{aligned}\mathbf{G}(t,\mathbf{x})&=\mathbf{G}_1(t,\mathbf{x}_1)+\mathbf{G}_2(t,\mathbf{x})\\&=\begin{bmatrix}0&0&0&-\frac{v}{\mathbf{B}}\\0&0&0&\mathbf{B}\mathbf{z}_1\end{bmatrix}+\begin{bmatrix}r&0&-\frac{\mathbf{B}}{\mathbf{A}}&0\\0&0&\mathbf{B}r&0\end{bmatrix}\\ \|\mathbf{G}_1(t,\mathbf{x}_1)\|_2&\le\max(\mathbf{B},\frac{1}{\mathbf{B}})\sqrt{(z_1^2+v^2)}\\&=\max(\mathbf{B},\frac{1}{\mathbf{B}})\|x_1\|_2\\&=\theta_1\|x_1\|_2\end{aligned}$$

and

$$\begin{aligned}\|\mathbf{G}_2(t,\mathbf{x})\|_2&\le(\mathbf{B}+1)\|r\|_2+\frac{\mathbf{B}}{\mathbf{A}}\le(\mathbf{B}+1)\|x_2\|_2+\frac{\mathbf{B}}{\mathbf{A}}\\&=\theta_2(\|x_2\|_2).\end{aligned}$$

The result follows from the norm property:

$$\|\mathbf{G}(t,\mathbf{x})\|_2\le\|\mathbf{G}_1(t,\mathbf{x}_1)\|_2+\|\mathbf{G}_2(t,\mathbf{x})\|_2.$$

■

To satisfy the second condition of Theorem 4.1, we thereafter need to design the control u in (40) that stabilizes (43). We will first transform (43) into a chained form, $\boldsymbol{\alpha}$ and r are considered as virtual inputs to the system. Applying the following change of coordinates:

$$\mathbf{y}_1=\mathbf{Z}_2 \tag{47}$$

$$\mathbf{y}_2=\boldsymbol{\alpha} \tag{48}$$

$$\mathbf{y}_3=\mathbf{z}_3 \tag{49}$$

$$\mathbf{u}_1=\tau_r,\qquad \mathbf{u}_2=\tau_\alpha \tag{50}$$

leads to the following triangular third-order chained form system:

$$\dot{\mathbf{y}}_1=\mathbf{y}_2\mathbf{u}_1 \tag{51}$$

$$\dot{\mathbf{y}}_2=\mathbf{u}_2 \tag{52}$$

$$\dot{\mathbf{y}}_3=\mathbf{u}_1. \tag{53}$$

System (51)–(53) violates Brockett's conditions to be stabilized by smooth time-invariant feedback stabilization [2]. Then, we suggest a backstepping approach to stabilize this triangular form to the origin.

Theorem 4.2: Consider system (51)–(53) with the following control laws:

$$\mathbf{u}_1=-\mathbf{k}_3\mathbf{y}_3 \tag{54}$$

$$\mathbf{u}_2=\mathbf{k}_3\mathbf{y}_1\mathbf{y}_3-(\mathbf{k}_1+\mathbf{k}_2)\mathbf{y}_2+\mathbf{k}_1\left(1+\frac{\mathbf{k}_2}{\mathbf{k}_3}\right)\frac{\mathbf{y}_1}{\mathbf{y}_3} \tag{55}$$

with $\mathbf{k}_3>0$, $\mathbf{k}_2>0$, and $\mathbf{k}_1>\mathbf{k}_3$.

1) The whole state $y=(\mathbf{Z}_2,\boldsymbol{\alpha}_2,\mathbf{z}_3)^\top$ is bounded and decays exponentially to zero when $t\to\infty$ for all $\mathbf{y}\in\Omega=\{(\mathbf{y}_1,\mathbf{y}_2,\mathbf{y}_3)\in\mathbb{R}^3|\mathbf{y}_3(t)\neq0,\forall t\ge0\}$;
2) The control law is well-defined and bounded for all $t>0$.

Proof: To make the last coordinate $\mathbf{y}_3$ exponentially stable, we use a linear state feedback $\mathbf{u}_1=-\mathbf{k}_3\mathbf{y}_3$, where $\mathbf{k}_3$ is a positive parameter. System (51)–(53) becomes

$$\dot{\mathbf{y}}_1=-\mathbf{k}_3\mathbf{y}_2\mathbf{y}_3 \tag{56}$$

$$\dot{\mathbf{y}}_2=\mathbf{u}_2 \tag{57}$$

$$\dot{\mathbf{y}}_3=-\mathbf{k}_3\mathbf{y}_3. \tag{58}$$

The problem consists in finding a control law $\mathbf{u}_2$ such that if the initial state belongs to set $\Omega=\{(\mathbf{y}_1,\mathbf{y}_2,\mathbf{y}_3)\in\mathbb{R}^3|\mathbf{y}_3(t)\neq0,\forall t\ge0\}$, the whole state of the closed-loop system remains bounded and converges exponentially to zero. The backstepping procedure is performed in two steps.

Step 1: Stabilization of the y_1-subsystem of (56).

Define the candidate Lyapunov function for the first (56), such that $V_1(\mathbf{y}_1)=\frac{1}{2}\mathbf{y}_1^2$. By considering $\mathbf{y}_2$ as a virtual control defined over the set $\Omega=\{(\mathbf{y}_1,\mathbf{y}_2,\mathbf{y}_3)\in\mathbb{R}^3|\mathbf{y}_3(t)\neq0,\forall t\ge0\}$. If we select $\mathbf{y}_2=\Psi_1(\mathbf{y}_1,\mathbf{y}_3)$, such that

$$\Psi_1(\mathbf{y}_1,\mathbf{y}_3)=\frac{\mathbf{k}_1}{\mathbf{k}_3}\frac{\mathbf{y}_1}{\mathbf{y}_3} \tag{59}$$

the time derivative of V_1 becomes

$$\dot{V}_1=-\mathbf{k}_1y_1^2,\qquad \mathbf{k}_1\ge0. \tag{60}$$

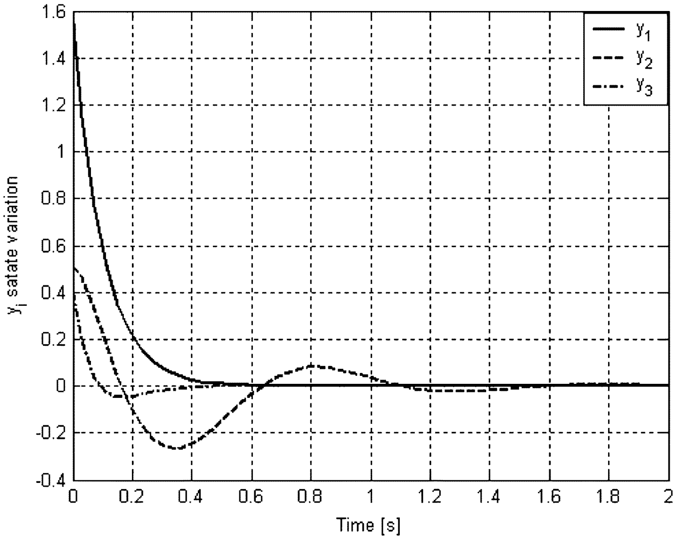

Fig. 2. Exponential convergence of the chained form (51)–(53).

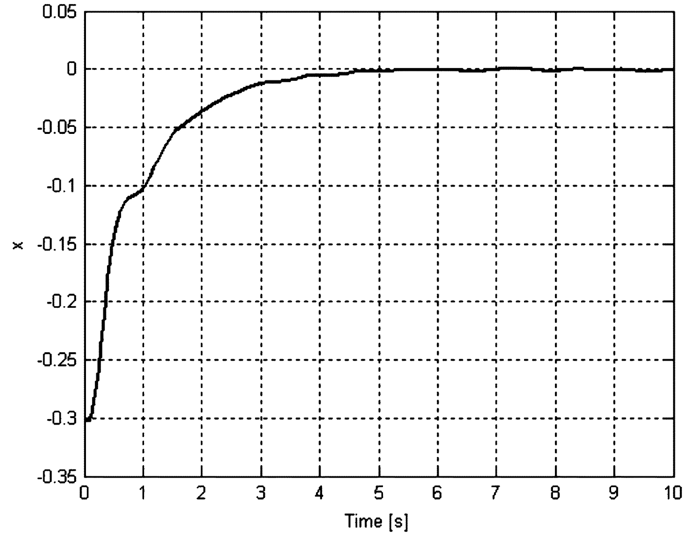

Fig. 3. Time evolution of the state x.

Step 2: Backstepping for y_2.

We introduce the new variable $\varpi_2 = \mathbf{y}_2 - \Psi_1(y_1, y_3)$, which represents the deviation of $\mathbf{y}_2$ from the virtual control Ψ_1, and consider in (57) and (58), where $\mathbf{y}_2$ is substituted by $\varpi_2 = \mathbf{y}_2 - \Psi_1(y_1, y_3)$

$$\dot{\mathbf{y}}_1 = -\mathbf{k}_3(\varpi_2 + \Psi_1)\mathbf{y}_3 \tag{61}$$

$$\dot{\varpi}_2 = \mathbf{u}_2 + \mathbf{k}_1(\varpi_2 + \Psi_1) - \mathbf{k}_1\frac{\mathbf{y}_1}{\mathbf{y}_3}. \tag{62}$$

Defining the Lyapunov function

$$V_2(y_1, y_2) = V_1(\mathbf{y}_1) + \frac{1}{2}\varpi_2^2 \tag{63}$$

the following control law defined over Ω:

$$\mathbf{u}_2 = \Psi_2(\mathbf{y}_1, \mathbf{y}_2, \mathbf{y}_3) = \mathbf{k}_3\mathbf{y}_1\mathbf{y}_3 - \mathbf{k}_1(\varpi_2 + \Psi_1) - \mathbf{k}_2\varpi_2 + \mathbf{k}_1\frac{\mathbf{y}_1}{\mathbf{y}_3}$$

leads to

$$\dot{V}_2 = -\mathbf{k}_1\mathbf{y}_1^2 - \mathbf{k}_2\varpi_2^2, \mathbf{k}_2 \geq 0. \tag{64}$$

Then, we can conclude that $\mathbf{y}_1$ and ϖ_2 are bounded and tend to zero as $t \to \infty$. Therefore, $\mathbf{y}_2$ tends to $(\mathbf{k}_1/\mathbf{k}_3)(\mathbf{y}_1/\mathbf{y}_3)$. To guarantee the boundedness and the convergence to zero of $\mathbf{y}_2$, we must ensure the boundedness and the convergence to zero of $\mathbf{y}_1/\mathbf{y}_3$ when $t \to \infty$. Noticing that

$$\dot{V}_1 = -2\mathbf{k}_1 V_1 \tag{65}$$

we can conclude that when $t \to \infty, V_1(t)$ decays to zero as $e^{-2\mathbf{k}_1 t}$, and $\mathbf{y}_1$ as $e^{-\mathbf{k}_1 t}$. Since $\mathbf{y}_3$ decays to zero as $e^{-\mathbf{k}_3 t}$, we then conclude that the ratio $(\mathbf{y}_1/\mathbf{y}_3)$ is bounded and decays to zero as $e^{-(\mathbf{k}_1 - \mathbf{k}_3)t}$, provided that $\mathbf{k}_1 > \mathbf{k}_3$ and $\mathbf{y}_3(0) \neq 0$. ■

Corollary 4.1: According to Theorem 4.1 and Propositions 4.1–4.2, the underactuated ship is uniformly globally asymptotically stabilized with the control law resulting from Theorem 4.2 and expressed in the original coordinates of the system by (66) and (67) at the bottom of the page.

Remark 1: Notice that selecting the gains $\mathbf{k}_i, i = 1, 2, 3$ which meet the conditions in Theorem 4.2, is feasible. The gain $\mathbf{k}_3$ could, for instance, be first chosen to achieve a satisfactory

$$\begin{aligned} x(0) &= -0.1979 \text{ m} \quad & \mathbf{z}_1(0) &= 0.8 \text{ m} \\ y(0) &= 0.8 \text{ m} \quad \Leftrightarrow & \mathbf{z}_2(0) &= 0.1979 \text{ m} \\ \psi(0) &= \pi/2 \text{ rad} & \mathbf{z}_3(0) &= 0 \text{ rad} \\ u(0) &= 1.6 \text{ m/s} & \mathbf{Z}_2(0) &= 0.4 \text{ m} \\ v(0) &= 0.1 \text{ m/s} & & \\ r(0) &= \frac{\pi}{2} \text{ rad/s} & & \end{aligned}$$

$$\tau_1 = \begin{cases} -d_{22}\Big[(r + \mathbf{k}_3\psi + \frac{c_2}{\psi})(-x\sin(\psi) + y\cos(\psi) + \frac{v}{\mathbf{B}}) & \\ (1 + c_1\frac{\mathbf{A}}{\mathbf{B}} - \frac{d_{11}}{d_{22}})u + c_1(x\cos(\psi) + y\sin(\psi))\Big] & \forall\psi(0) \neq 0 \\ -\frac{\mathbf{B}}{\mathbf{A}}(\tau_\alpha^* + r^* + u) & \forall\psi(0) = 0 \end{cases} \tag{66}$$

$$\tau_3 = \begin{cases} (m_{22} - m_{11})uv + (d_{33} - m_{33}\mathbf{k}_3)r & \forall\psi(0) \neq 0 \\ (m_{22} - m_{11})uv + d_{33}r^* & \forall\psi(0) = 0 \end{cases} \tag{67}$$

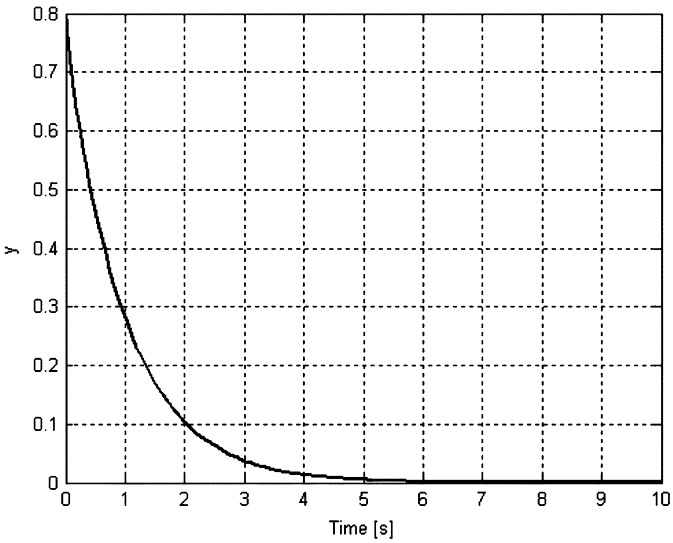

Fig. 4. Time evolution of the state y.

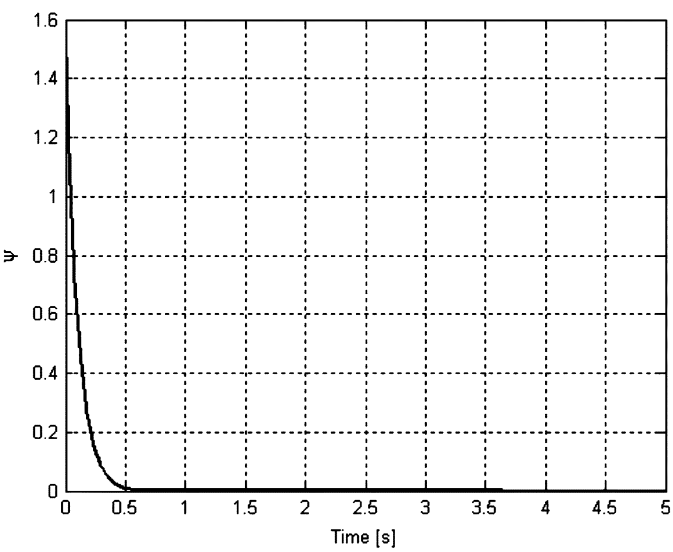

Fig. 5. Time evolution of the yaw angle.

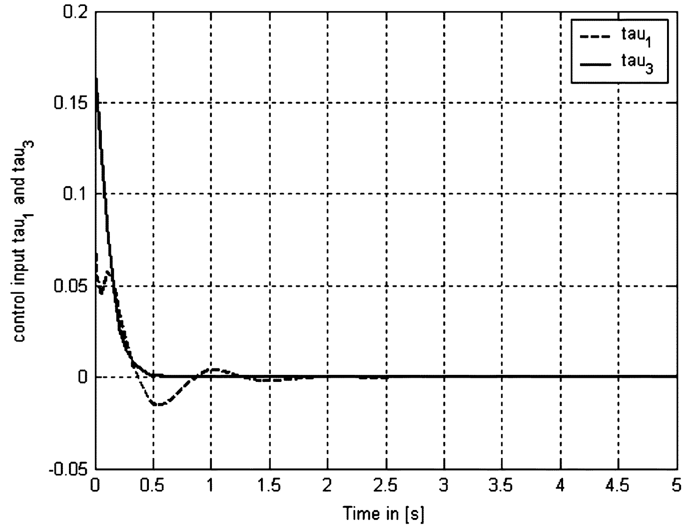

Fig. 6. Time evolution of the control inputs τ_1 and τ_3.

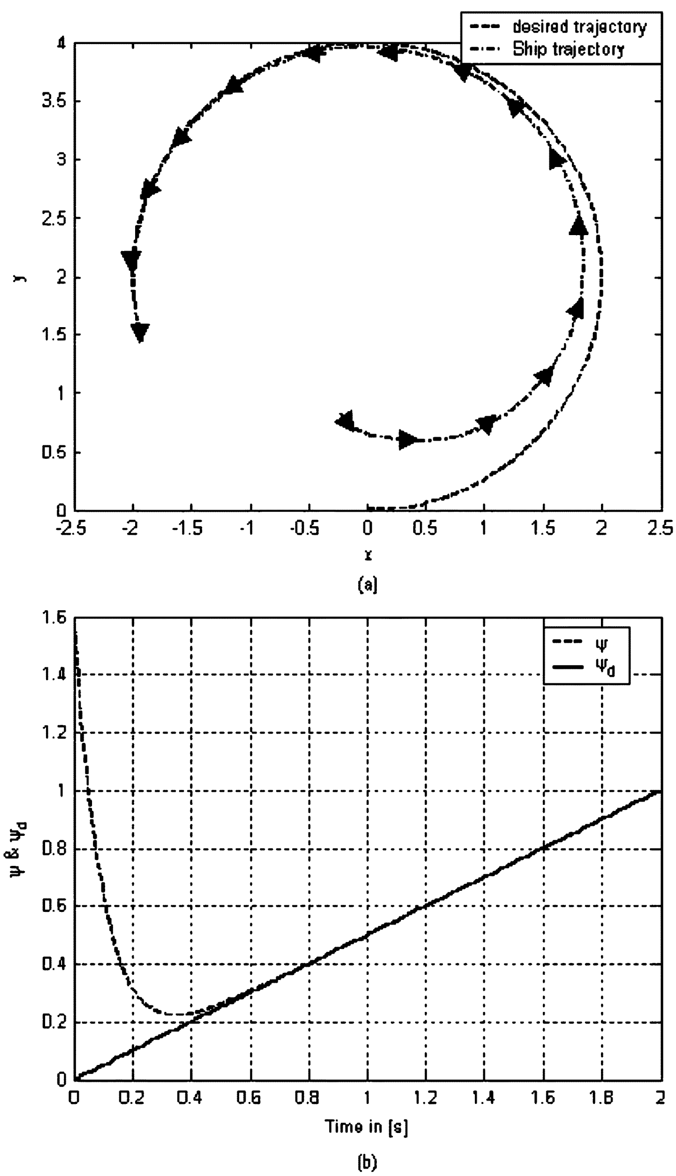

Fig. 7. (a) Actual and reference trajectory. (b) Time evolution of the actual heading angle and its reference.

dynamics of the state $\mathbf{y}_3$, and, hence, of $\mathbf{z}_3$. The ratio $(\mathbf{y}_1/\mathbf{y}_3)$ provides the condition on $\mathbf{k}_1$ that would be selected as $\mathbf{k}_1 = 2\mathbf{k}_3$ if we wish that $\mathbf{y}_3$ and $\mathbf{y}_1$ converge with similar dynamic performance. The required value for $\mathbf{k}_2$ can, therefore, be adjusted so as to have a satisfactory dynamic response for $\mathbf{y}_2$ but also to guarantee faster dynamics for ψ compared to those of x and y.

Remark 2: The proposed control law for subsystem $\sum_2$ guarantees the boundedness of the whole state and makes the origin of the closed-loop chained system exponentially attractive provided that the initial states belong to the set $\Omega = \{(\mathbf{y}_1, \mathbf{y}_2, \mathbf{y}_3) \in \mathbb{R}^3 | \mathbf{y}_3(t) \neq 0, \forall t \geq 0\}$. If the system starts outside Ω, we apply an open-loop control for an arbitrarily small time to drive the system away from $\mathbf{y}_3 = 0$ and then switch to the state feedback control law.

Note that the control laws (66)–(67) result in a static state feedback, that can easily be implemented, provided that the states of the system are available.

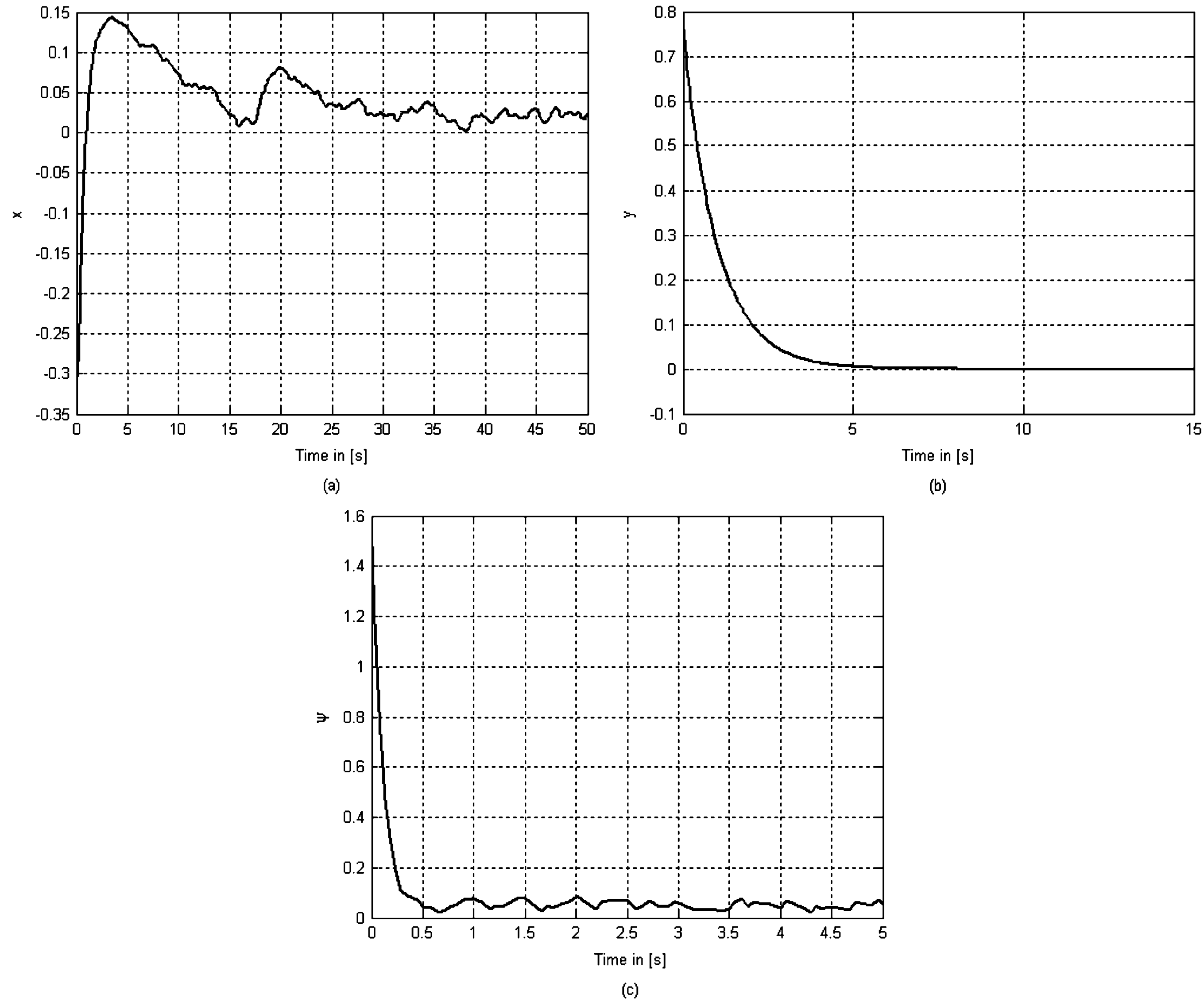

Fig. 8. (a) Time evolution of the state x under external disturbances. (b) Time evolution of the state y under external disturbances. (c) Time evolution of the state ψ under external disturbances.

IV. Simulation Results

Fig. 2 shows the exponential stabilization of the chained form (51)–(53) under control law (54) and (55). The controller parameters used were $\mathbf{k}_1 = 10, \mathbf{k}_2 = 5, \mathbf{k}_3 = 5$. To test the convergence of the complete system, a model of cybership I [10] of the laboratory of Norwegian University of Science and Technology (NTNU), Trondheim, Norway, was considered, for which the normalized parameters are $m_{11} = 19.0$, $m_{22} = 35.2$, $m_{33} = 4.2$, $d_{11} = 4.0$, $d_{22} = 10.0$, $d_{33} = 1.0$. The initial states considered in the simulations are shown in equations (66) and (67) at the bottom of the page, with $c_1 = \mathbf{k}_1 + \mathbf{k}_2$ and $c_2 = \mathbf{k}_1(1 + \mathbf{k}_2/\mathbf{k}_3), r^* \in \mathbb{R} - \{0\}$ and $\tau_\alpha^* \in \mathbb{R} - \{0\}$ are two constant values.

Simulations of the complete system were made using the system (34)–(38) under the controller (66)–(67). Figs. 3–6 show the time evolution of the original state variables (x, y, ψ) and the torques (τ_1, τ_3). As expected, simulations reveal that the vessel converges globally uniformly to the origin with acceptable dynamic performances. It can be observed that the dynamics of ψ is much faster than those of x and y which makes sense in practice. Moreover, system outputs as well as control variables, do not present chattering and/or oscillatory behaviors.

Extension for Trajectory Tracking: It can be seen that the control laws (66) and (67) can be extended to perform the trajectory tracking of the state vector $\eta = [x, y, \psi]^T$ to a desired position vector $\eta_d = [x_d, y_d, \psi_d]^T$. This can be achieved simply by writing (14) as follows:

$$\mathbf{z}_1 = (x - x_d)\cos(\psi) + (y - y_d)\sin(\psi) \tag{68}$$

$$\mathbf{z}_2 = -(x - x_d)\sin(\psi) + (y - y_d)\cos(\psi) \tag{69}$$

$$\mathbf{z}_3 = \psi - \psi_d. \tag{70}$$

For a circular desired trajectory, the desired position η_d must satisfy the following equations:

$$\dot{x}_d = u_r\cos(\psi_d) \tag{71}$$

$$\dot{y}_d = u_r\sin(\psi_d) \tag{72}$$

$$\dot{\psi}_d = r_r \tag{73}$$

$$v_r = 0. \tag{74}$$

To simulate the behavior of the system, we set the desired linear and angular speed to $u_r = 0.5$ m/s and $r_r = 0.5$ rad/s, respectively. The origin is considered as the initial state of the reference model (68)–(73). Fig. 7(a) shows the trajectory of the ship together with the reference trajectory, in the xy-plane. Fig. 7(b) shows the time-evolution of the yaw angle together with the desired yaw angle. It is clear from both figures that the trajectory tracking is successfully achieved.

Robustness Issues: When the ship is assumed to be exposed to external random perturbations like environmental disturbances, the controlled ship is demonstrated to possess some robustness properties. Fig. 8(a)–(c) shows the simulation results when environmental disturbances, assumed to be random noise with magnitude of 1 and 0 lower bound, are added to the system. In this case, the convergence is illustrated to be bounded by a neighborhood of the origin (small-signal L_∞ stability).

V. Conclusion

In this brief, the control problem of uniform global stabilization and tracking of an underactuated surface vessel has been considered. A discontinuous feedback control law has been derived using a backstepping approach. We have shown that the original coordinates of the controlled vessel converges globally uniformly asymptotically to the origin. Simulations results have revealed that the control objectives are achieved with acceptable dynamic performance.

Future research directions would address the robust/adaptive control problem of underactuated ships subjected to external disturbances and model uncertainties.

References

[1] A. Astolfi, “Exponential stabilization of nonholonomic systems via discontinuous control,” in *Proc. Symp. Nonliner Contr. Syst. Des.*, 1995, pp. 741–746.

[2] R. Brockett, “Asymptotic stability and feedback stabilization,” in *Differential Geometric Control Theory*. Boston, MA: Birkhauser, 1983, pp. 181–191.

[3] F. Bullo, N. E. Leonard, and A. D. Lewis, “Controllability and motion algorithms for underactuated lagrangian systems on lie groups,” *IEEE Trans. Autom. Contr.*, vol. 45, no. 8, pp. 1437–1454, Aug. 2000.

[4] C. Byrnes and A. Isidori, “On the attitude stabilization of rigid spacecraft,” *Automatica*, vol. 27, pp. 87–95, 1991.

[5] P. E. Crouch, “Spacecraft attitude control and stabilization: Applications of geometric control theory to rigid body models,” *IEEE Trans. Autom. Contr.*, vol. 29, no. 4, pp. 321–331, Apr. 1984.

[6] I. Fantoni, R. Lozano, F. Mazenc, and K. Y. Pettersen, “Stabilization of a nonlinear underactuated hovercraft,” *Int. J. Robust Nonlinear Contr.*, vol. 10, no. 8, pp. 645–654, 2000.

[7] M. Fliess, J. Levine, P. Martin, and P. Rouchon, “Flatness and defect of nonlinear systems: Introductory theory and example,” *Int. J. Contr.*, vol. 61, no. 9, pp. 1327–1361, 1995.

[8] T. I. Fossen, *Guidance and Control of Ocean Vehicles*. New York: Wiley Interscience, 1994.

[9] J. M. Godhavn, “Topics in nonlinear motion control: Nonholonomic, underactuated, and hybrid systems,” Ph.D. dissertation, Dept. Eng. Cybernetics, Norwegian Univ. Sci. Technol., Trondheim, Norway, 1997.

[10] E. Lefeber, A. Robertsson, and H. Nijmeijer, “Linear controllers for exponential tracking of systems in chained-form,” *Int. J. Robust Nonlinear Contr.*, pp. 243–263, 2000.

[11] F. Mazenc, K. Y. Pettersen, and H. Nijmeijer, “Global uniform asymptotic stabilization of an underactuated surface vessel,” in *Proc. 41st IEEE Conf. Dec. Contr.*, 2002, pp. 510–515.

[12] R. Murray and S. Sastry, “Nonholonomic motion planning: Steering using sinusoids,” *IEEE Trans. Autom. Contr.*, vol. 38, no. 5, pp. 700–716, May 1992.

[13] S. Olfati, “Nonlinear Control of underactuated mechanical systems with application to robotics and aerospace vehicles,” Ph.D. dissertation, Dept. Elect. Eng. Comp. Sci., Massachusetts Inst. Technol., Cambridge, Feb. 2001.

[14] G. Oriolo and Y. Nakamura, “Free-Joint manipulators: Motion control under second order nonholonomic constraints,” in *IEEE/RSJ Int. Workshop Intelligent Robots Syst.*, 1991, pp. 1248–1253.

[15] E. Panteley and A. Loria, “Global uniform asymptotic stability of cascade time-varying nonlinear systems: Case study,” in *Proc. 35th IEEE Conf. Dec. Contr.*, 1996, pp. 590–591.

[16] K. Y. Pettersen, “Exponential Stabilization of Underactuated Vehicles,” Ph.D. dissertation, Norwegian Univ. Sci. Technol., Trondheim, Norway, 1996.

[17] K. Y. Pettersen and O. Egeland, “Exponential stabilization of an underactuated surface vessel,” in *Proc. 35th IEEE Conf. Dec. Contr.*, 1996, pp. 967–971.

[18] K. Y. Pettersen and H. Nijmeijer, “Global practical stabilization and tracking for an underactuated ship: A combined averaging and backstepping approach,” in *Proc. IFAC Conf. Syst. Structure Contr.*, 1998, pp. 59–64.

[19] M. Reyhanoglu, “Control and stabilization of an underactuated surface vessel,” in *Proc. 35th IEEE Conf. Dec. Contr.*, 1996, pp. 2371–2376.

[20] H. J. Sussmann, “Subanalytic sets and feedback control,” *J. Differential Equations*, vol. 31, pp. 31–52, 1979.

[21] K. Y. Wichlund, O. Srdalen, and O. Egeland, “Control properties of underactuated vehicles,” in *Proc. IEEE Int. Conf. Robot. Autom.*, 1995, pp. 2009–2014.